Optic Tamm states: The Bloch-wave-expansion method

Xiubao Kang, Wei Tan, Zhiguo Wang,* and Hong Chen
Pohl Institute of Solid State Physics, Tongji University, Shanghai 200092, People's Republic of China
(Received 13 January 2009; published 29 April 2009)

Optic Tamm states (OTSs) in one-dimensional photonic crystal (PhC) heterostructures are studied via a Bloch-wave-expansion method (BWEM). We show that by considering both the periodicity and the finiteness, the propagation of electromagnetic wave in a finite one-dimensional PhC can be characterized by three parameters—two Bloch impedances and the Bloch-wave vector—in the framework of the BWEM. Applying the BWEM, we give a criterion of optic Tamm states at the interfaces inside finite heterostructures. It is demonstrated that the criterion is applicable for the OTSs at the interface inside both finite PhC-PhC heterostructures and PhC-metal heterostructures. In addition, we also discuss the importance of the number and the element order of the unit cells in the occurrence of optic Tamm states.

DOI: 10.1103/PhysRevA.79.043832 PACS number(s): 42.70.Qs, 78.67.Pt, 73.20.At, 41.20.Jb

I. INTRODUCTION

Electromagnetic (EM) surface wave is the wave that is confined at the interface between two different media [1]. One of the most well-known surface waves is the surface plasmons (SPs) which can be excited at the interface of metal and homogeneous dielectrics [2,3]. The wide applications of SPs include subwavelength microscopy, agent sensing, enhanced light-matter interaction, etc. [4–6]. Due to the special dispersions of the SPs which lie outside of the light cone, they can only be excited by near fields. It is needed to seek help from the attenuated total reflection or other configurations [3], while these configurations are not always convenient in experiments or device designs. In addition, the absorption in the metal is another factor that hinders the SPs from more applications. Recently, optic Tamm states (OTSs) [7] occurring at the interfaces inside one-dimensional (1D) photonic crystal (PhC) heterostructures have drawn much attention [7–18]. Unlike the cases of SPs where the EM fields are confined to the interface by the total internal reflection in the dielectric, fields of the OTSs decay away from the interface in the PhCs due to the Bragg reflection. The dispersions of the OTSs are not required to lie outside of the light cone and thus OTSs can be excited directly by propagating modes. Furthermore, as the absorption of dielectrics is much lower than that of metals, OTSs at the interface between two PhCs will not suffer from severe loss as in SPs. The ease of realization and some intrinsic natures of OTSs bring many potential applications such as the fabrication of polariton lasers [8], magnetotunable filters [9], and thermophotovoltaic devices [10].

Predictions about the occurrence of OTSs in the PhC heterostructures are of special importance. Most of the previous theoretical studies focus on OTSs in heterostructures composed by two semi-infinite PhCs [6,11–13]. However, real structures are all finite and the advent of the boundaries makes the EM fields different from those inside infinite structures. The predictions made in previous works fit the results well for cases, where the numbers of unit cells are large enough, but do not fit well when the numbers are small. However, in experiments about OTSs, the numbers of the unit cells in PhCs are small (see, e.g., in [9,10]) and thus the effect of the boundaries is no longer ignorable. Reference [18] extended the parameter retrieval method [19] to the descriptions of finite PhCs and analogized the OTSs with the interface modes at the interface of two single-negative mediums [20]. As a homogenization procedure, the parameter retrieval method characterizes a finite PhC by the parameters retrieved from the global transmittance and reflectance. However, the different physics in PhCs and homogeneous materials limits the method to PhCs with special unit-cell configurations. Unfortunately, in most studies about OTSs, the unit cells of the PhCs are of the wavelength scale and are often asymmetric [6,8–17]. It is known that the parameter retrieval procedure is however counterproductive for such structures [19].

Considering the finiteness of the practical PhCs and taking advantage of the periodicity, we introduce a Bloch-wave-expansion method (BWEM) to the study of OTSs in this paper. In the framework of the BWEM, EM field inside a finite PhC is expanded as a combination of Bloch waves propagating in contrary directions. By the introduction of two Bloch impedances, the global transmission properties of 1D PhCs with any unit-cell configurations can be presented in a simple way. When applying the BWEM into the study of EM fields in a PhC heterostructure, analytical predictions about OTSs can be easily obtained. The derived analytical occurrence condition of the OTSs is in a quite simple form, which provides us the great convenience in designing OTSs or discussing the mechanism involved. In the studies about intermediate-mode-assisted optical coupler, EM fields in finite waveguide arrays are calculated by a similar Bloch-wave-expansion approach [21] and the results have been compared with those calculated in the framework of the paraxial approximation [22]. It is shown that the result from the Bloch-wave approach is accurate. The rest of the paper is organized as follows. In Sec. II, basing on the Bloch-Floquet theorem, we present the BWEM for 1D finite PhCs. Applying the BWEM, in Sec. III, we give a criterion of optic Tamm states at the interfaces inside finite PhC-PhC heterostructures and demonstrate that the criterion is also applicable for the OTSs at the interface inside PhC-metal hetero-

*Corresponding author; zgwang@mail.tongji.edu.cn

structures. Finally, the discussion and conclusion are given in Sec. IV.

II. BLOCH-WAVE-EXPANSION METHOD

Monochromatic EM waves in infinite periodic structures obey the Bloch-Floquet theorem and take the forms of Bloch waves. For 1D PhCs with permittivity periodically modulated along the z direction, the transverse (along x-y plane) components of electromagnetic fields of a Bloch wave can be expressed by a two-element column vector as $e^{\pm ilk^{\mathrm{Bloch}}\cdot d+ik_x x+ik_y y-i\omega t}\begin{bmatrix}E(z)\\H(z)\end{bmatrix}$ where k^{Bloch} is the Bloch-wave vector, k_x and k_y are the transverse components of the wave vector, $E(z)$ and $H(z)$ are periodic functions, respectively, in dimensions of electric and magnetic fields, and d is the lattice constant. At the position of lth unit-cell surfaces z_l, the column vector $\begin{bmatrix}E(z_l)\\H(z_l)\end{bmatrix}$ fulfills [23]

$$\hat{T}\times\begin{bmatrix}E(z_l)\\H(z_l)\end{bmatrix}=e^{\pm ik^{\mathrm{Bloch}}\cdot d}\begin{bmatrix}E(z_l)\\H(z_l)\end{bmatrix}. \tag{1}$$

Here, $\hat{T}$ is the translation operator across one unit cell. For the case of typical binary unit-cell configuration (AB), the translation operator takes the form of a 2×2 matrix T with elements [19]

$$T(1,1)=\cos k_A d_A\cos k_B d_B-\frac{\xi_B}{\xi_A}\sin k_A d_A\sin k_B d_B,$$

$$T(1,2)=i\xi_A\sin k_A d_A\cos k_B d_B+i\xi_B\cos k_A d_A\sin k_B d_B,$$

$$T(2,1)=i\frac{1}{\xi_A}\sin k_A d_A\cos k_B d_B+i\frac{1}{\xi_B}\cos k_A d_A\sin k_B d_B,$$

$$T(2,2)=\cos k_A d_A\cos k_B d_B-\frac{\xi_A}{\xi_B}\sin k_A d_A\sin k_B d_B. \tag{2}$$

Here, $d_i(i=A,B)$ corresponds to the thickness of layers A or B, $k_i=\sqrt{\varepsilon_i k_0^2-k_x^2-k_y^2}$ is the normalized wave vector in the corresponding dielectric layers with a permittivity ε_i, $\xi_i=\frac{\omega\mu_0}{k_i}$ is the normalized wave impedance for TE waves and $\xi_i=\frac{k_i}{\omega\varepsilon_i}$ for TM waves. One of the most different features between OTSs and SPs is that OTSs can be excited directly by normally incident propagating modes; we focus on the cases of normal incidence in the following.

The dispersion relation of the infinite PhCs can be obtained by solving the trace of the transfer matrix T,

$$\cos k^{\mathrm{Bloch}}d=\frac{\mathrm{tr}(T)}{2}. \tag{3}$$

Equation (1) is an eigenequation and $e^{ik^{\mathrm{Bloch}}d}$ or $e^{-ik^{\mathrm{Bloch}}d}$ is the eigenvalue where $k^{\mathrm{Bloch}}d$ or $-k^{\mathrm{Bloch}}d$ depicts the phase change in Bloch waves across one unit cell in positive or negative direction. The column vector $\begin{bmatrix}E(z_l)\\H(z_l)\end{bmatrix}$ is one of the two eigenvectors of the transfer matrix [24,25]. Extracting $H(z_l)$ from the column vector $\begin{bmatrix}E(z_l)\\H(z_l)\end{bmatrix}$ and removing the $H(z_l)$ from both sides of Eq. (1), we obtain the eigenequation corresponding to PhCs with binary unit-cell configuration (AB) in the following form:

$$T\times\begin{bmatrix}\xi_{\pm}^{\mathrm{Bloch}}\\1\end{bmatrix}=e^{\pm ik^{\mathrm{Bloch}}d}\begin{bmatrix}\xi_{\pm}^{\mathrm{Bloch}}\\1\end{bmatrix}, \tag{4}$$

where the characteristic parameters $\xi_{\pm}^{\mathrm{Bloch}}$, which are the ratios between the electric fields and the magnetic fields of Bloch wave propagating in, respectively, positive and negative directions, can be referred as Bloch impedances pertaining to corresponding PhCs. The column vectors

$$\begin{bmatrix}\xi_{\pm}^{\mathrm{Bloch}}\\1\end{bmatrix}$$

are the eigenvectors of the transfer matrix corresponding, respectively, to the eigenvalues $e^{ik^{\mathrm{Bloch}}d}$ and $e^{-ik^{\mathrm{Bloch}}d}$. For frequencies lying in the odd band or the odd gap, the Bloch impedances in the case of the binary unit-cell configuration (AB) is

$$\xi_{\pm}^{\mathrm{Bloch}}=\frac{\mp 2\xi_A\xi_B\sqrt{1-\cos^2 k^{\mathrm{Bloch}}d}-i(\xi_A^2-\xi_B^2)\sin k_A d_A\sin k_B d_B}{(\xi_B-\xi_A)\sin(k_A d_A-k_B d_B)+(\xi_B+\xi_A)\sin(k_A d_A+k_B d_B)}. \tag{5}$$

In even band or even gap, the sign "$\mp$" should be changed to "$\pm$" on the right-hand side of Eq. (5).

These two impedances are of vital importance in describing the transmission properties of the PhCs. An important point one should notice is that at (AB) interface, EM waves propagating in opposite directions see different unit-cell configurations [(AB) or (BA)]. By exchanging the position of ξ_A and ξ_B on the right-hand side of Eq. (5), one can get the Bloch impedances for (BA) unit cell as $\xi_{\pm}^{\mathrm{Bloch}'}=-\xi_{\mp}^{\mathrm{Bloch}}$. It is easy to understand that this conclusion can be extended to PhCs with arbitrary unit-cell configurations.

In the discussion of the electromagnetic parameter retrieval method, Ref. [19] has introduced two impedances in Eq. (35). It is obvious that two impedances are the Bloch impedances of the periodic structures. Comparisons between impedances of homogeneous materials and the Bloch impedances of periodic structures were made there. However, the lack of a unique definition of the Bloch impedances limits the rigorous homogenization procedure to periodic structures with symmetry unit-cell configurations.

In finite PhCs, the translation symmetry is broken by the advent of the external boundaries. When EM waves are impinging from one boundary, the two-element column vectors representing fields at the interfaces of unit cells do not take the form of a single eigenvector as expressed in Eq. (1) any more. A finite PhC with the same unit-cell configuration as the infinite case discussed above is shown in Fig. 1 and the coordinates of the surfaces of the unit cells are labeled with $z_1, z_2, \ldots z_j, \ldots z_n$. As

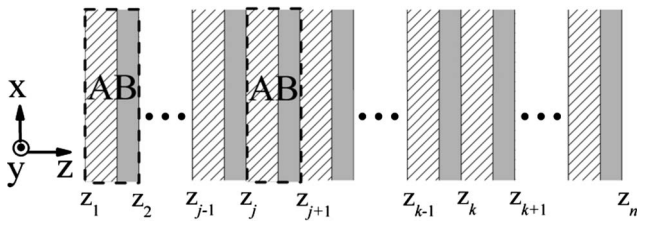

FIG. 1. 1D finite PhC with binary unit-cell configurations. The shaded (hatched) regions represent $A(B)$ layers. The squares with dashed border show two units. The positions that labeled with $z_1, z_2, \ldots z_j, \ldots z_n$ are the (AB) unit-cell surfaces.

$$\begin{bmatrix} \xi_+^{\text{Bloch}} \\ 1 \end{bmatrix}$$

and

$$\begin{bmatrix} \xi_-^{\text{Bloch}} \\ 1 \end{bmatrix}$$

are eigenvectors belonging to different eigenvalues of the same matrix, they are linear irrelevant and composing a complete basis set. We can decompose the column vector representing the fields at the jth unit-cell surface (z_j) into

$$\begin{bmatrix} E(z_j) \\ H(z_j) \end{bmatrix} = H_+ \begin{bmatrix} \xi_+^{\text{Bloch}} \\ 1 \end{bmatrix} + H_- \begin{bmatrix} \xi_-^{\text{Bloch}} \\ 1 \end{bmatrix}, \tag{6}$$

where H_+ and H_- are the complex coefficients in the dimension of the magnetic field. By the transfer-matrix method [19,26], we can achieve the column vector of EM fields at kth unit-cell surface (z_k) from that at jth unit-cell surface,

$$\begin{bmatrix} E(z_k) \\ H(z_k) \end{bmatrix} = (T)^{k-j} \begin{bmatrix} E(z_j) \\ H(z_j) \end{bmatrix}. \tag{7}$$

Combining Eqs. (6) and (7), we get

$$\begin{bmatrix} E(z_k) \\ H(z_k) \end{bmatrix} = H_+ (T)^{k-j} \begin{bmatrix} \xi_+^{\text{Bloch}} \\ 1 \end{bmatrix} + H_- (T)^{k-j} \begin{bmatrix} \xi_-^{\text{Bloch}} \\ 1 \end{bmatrix}. \tag{8}$$

Then we insert the eigenequation (4) into Eq. (8),

$$\begin{bmatrix} E(z_k) \\ H(z_k) \end{bmatrix} = H_+ e^{i(k-j)k^{\text{Bloch}}d} \begin{bmatrix} \xi_+^{\text{Bloch}} \\ 1 \end{bmatrix} + H_- e^{-i(k-j)k^{\text{Bloch}}d} \begin{bmatrix} \xi_-^{\text{Bloch}} \\ 1 \end{bmatrix}. \tag{9}$$

One can find from Eq. (9) that each part at the right-hand side of Eq. (6) propagates through k-j unit cell in the same manner as a Bloch wave propagating in one direction. This is in agreement with the argument that both finite and infinite periodic structures support the propagation of Bloch waves (see [27] and references therein). Now, it is convenient to get the transmission and reflection properties of a finite PhC by matching the fields at the two outer boundaries with those in the substrate.

In the derivation of the transfer matrix for a homogeneous slab in the traditional transfer-matrix algorithm, fields in the slab are usually studied by plane-wave-expansion methods [24]. When the whole space is filled with the same material, EM waves take the form of plane waves and the ratio between the electric field and the magnetic field equals to the impedance of the material. In terms of the column vector representation, fields of a plane wave inside a homogeneous material with impedance ξ_h and refractive index n can be represented by a two-element column vector of

$$H_h e^{ink_0 z} \begin{bmatrix} \xi_h \\ 1 \end{bmatrix}$$

or

$$H_h e^{-ink_0 z} \begin{bmatrix} -\xi_h \\ 1 \end{bmatrix}$$

which represents EM plane waves propagating in one direction, along positive z or negative z direction. Here, k_0 is the wave vector in free space, H_h is the magnetic field, and

$$\begin{bmatrix} \xi_h \\ 1 \end{bmatrix}$$

and

$$\begin{bmatrix} -\xi_h \\ 1 \end{bmatrix}$$

are the plane-wave eigenstates of the infinite homogeneous material. When it comes to the cases of a finite slab, plane waves experience multireflections due to the advent of the external boundaries. Fields inside finite slabs do not take the form of a plane wave propagating in a single direction as before. In traditional plane-wave-expansion methods, they are considered as superposition of two contrary propagating plane waves. The column vectors of fields can be expressed as

$$\begin{bmatrix} E(z) \\ H(z) \end{bmatrix} = H_{h+} e^{ink_0 z} \begin{bmatrix} \xi_h \\ 1 \end{bmatrix} + H_{h-} e^{-ink_0 z} \begin{bmatrix} \xi_h \\ 1 \end{bmatrix}. \tag{10}$$

The differences between Eqs. (9) and (10) are (i) functions on the right-hand sides of these two equations represent, respectively, Bloch and plane waves and (ii) the eigenimpedances in BWEM are $\xi_\pm^{\text{Bloch}}$ while those in-plane-wave expansion method are $\pm\xi_h$. For a 1D PhC with symmetric unit cell configurations, we can assign a $\xi_{\text{eff}} = \xi_+^{\text{Bloch}} = -\xi_-^{\text{Bloch}}$, which shows some similarity between 1D symmetric PhC and homogeneous slabs. Following the name of the plane-wave expansion methods, we call the expansion of field in the finite PhCs Bloch-wave-expansion method.

In plane-wave-expansion methods, the transmission properties of a homogeneous material are characterized by two parameters (ξ_h and nk_0). The BWEM uses three parameters (ξ_+^{Bloch}, ξ_-^{Bloch}, and k^{Bloch}) to describe the transmission properties of 1D PhCs. k^{Bloch}/k_0 is the effective refractive index. The need for two impedances (ξ_+^{Bloch} and ξ_-^{Bloch}) should be attributed to the lack of the reversal symmetry for PhCs with general unit-cell configurations.

III. CRITERION FOR THE OCCURRENCE OF OTSs

Here, we apply the BWEM to the study of the occurrence of OTSs. A typical heterostructure $[(AB)_m(CD)_n]$ is demon-

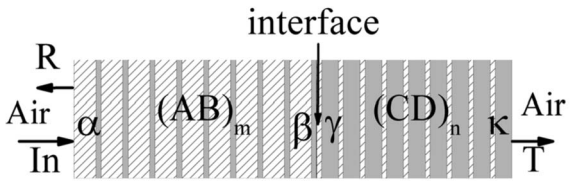

FIG. 2. A heterostructure and the surfaces of each constituting PhC. The surfaces are labeled, respectively, as α, β, γ, and κ.

strated in Fig. 2. The indexes m and n are, respectively, the numbers of unit cells in corresponding PhC slabs. The structure is embedded in free space with impedance ξ_0. For the sake of clarity, we define the front (left) and the behind (right) surfaces of the $(AB)_m[(CD)_n]$ slab as $\alpha\,[\gamma]$ and $\beta\,[\kappa]$, respectively. Correspondingly, ξ_i^s ($i=\alpha$, β, γ, or κ) presents the surface impedance which is the ratio between the electric field and magnetic field at surface i,

$$\xi_i^s = \frac{E_i}{H_i}. \tag{11}$$

As shown in Refs. [6,11,17], OTSs are characterized by a resonant tunneling or a perfect transmission. Thus for EM waves with the frequency of OTSs impinging from left, the reflection from the embedded heterostructures should be zero. As a direct consequence of the zero reflection, there should be $\xi_\alpha^s=\xi_0$ (α is the incident surface). At the right-hand side of the heterostructure, we have $\xi_\kappa^s=\xi_0$. The EM fields at the α and κ surfaces can be expressed as

$$H_\alpha \begin{bmatrix} \xi_0 \\ 1 \end{bmatrix} \text{ and } H_\kappa \begin{bmatrix} \xi_0 \\ 1 \end{bmatrix}, \tag{12}$$

where H_α and H_κ denote the complex tangential magnetic fields at corresponding surfaces. The surface impedances on both sides of the interface ξ_β^s and ξ_γ^s can be, respectively, calculated following Eqs. (6)–(9) as

$$\xi_\beta^s = \frac{\xi_{1+}^{\text{Bloch}} e^{imk_1^{\text{Bloch}}d_1}(\xi_0 - \xi_{1-}^{\text{Bloch}}) + \xi_{1+}^{\text{Bloch}} e^{-imk_1^{\text{Bloch}}d_1}(\xi_{1+}^{\text{Bloch}} - \xi_0)}{e^{imk_1^{\text{Bloch}}d_1}(\xi_0 - \xi_{1-}^{\text{Bloch}}) + e^{-imk_1^{\text{Bloch}}d_1}(\xi_{1+}^{\text{Bloch}} - \xi_0)}, \tag{13}$$

$$\xi_\gamma^s = \frac{\xi_{2+}^{\text{Bloch}} e^{-ink_2^{\text{Bloch}}d_2}(\xi_0 - \xi_{2-}^{\text{Bloch}}) + \xi_{2-}^{\text{Bloch}} e^{ink_2^{\text{Bloch}}d_2}(\xi_{2+}^{\text{Bloch}} - \xi_0)}{e^{-ink_2^{\text{Bloch}}d_2}(\xi_0 - \xi_{2-}^{\text{Bloch}}) + e^{ink_2^{\text{Bloch}}d_2}(\xi_{2+}^{\text{Bloch}} - \xi_0)}, \tag{14}$$

where the subscripts "1" and "2" designate, respectively, the left PhC $[(AB)_m]$ and right PhC $[(CD)_n]$, and $\xi_{i\pm}^{\text{Bloch}}$ ($i=1,2$) are the corresponding Bloch impedances [Eq. (5)]. Applying the boundary condition at the interface, the zero reflection can be reached when and only when

$$|\xi_\beta^s - \xi_\gamma^s| = 0 \tag{15}$$

is fulfilled [20]. Here, "$|\cdots|$" means the absolute value or the modulus of corresponding value. We take Eq. (15) as the criterion for OTSs in 1D PhC heterostructures. In general,

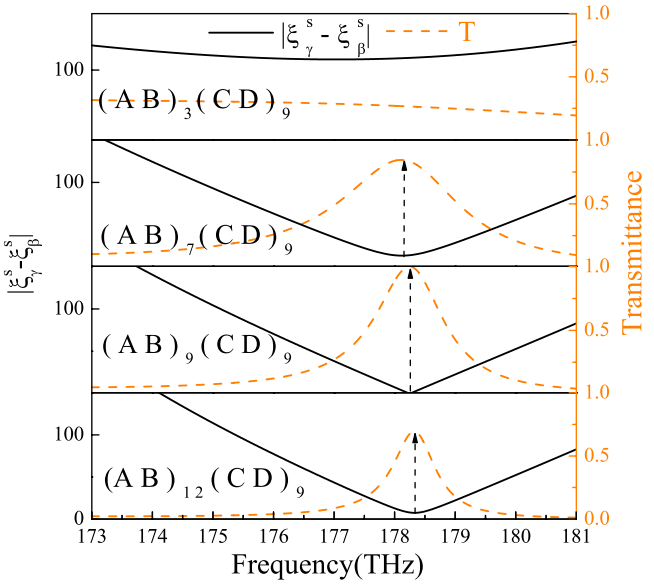

FIG. 3. (Color online) The matches of surface impedances and the transmittances for four heterostructures. The solid line in each subplot is $|\xi_\gamma^s - \xi_\beta^s|$ and the dashed line represents the corresponding transmittance (t). The parameters of the corresponding layers are $\varepsilon_A=\varepsilon_C=1.96$ and $\varepsilon_B=\varepsilon_D=4$; $d_A=435.5$ nm, $d_B=96$ nm, $d_C=100$ nm, and $d_D=330$ nm.

not all cases satisfying Eq. (15) are OTSs. In the frequency range lying in the band of both constituting PhCs, there are also complete transmissions (zero reflections). As OTS is a kind of resonant tunneling, it only appears in the gaps of both constituting PhCs. Once Eq. (15) is fulfilled in such frequency range, OTS appears.

A comparison between the frequency of the OTS derived from the surface impedances matching condition and the frequency of the transmission peak of heterostructures $(AB)_m(CD)_n$ is shown in Fig. 3. The relative dielectric constants of constituting layers are chosen as $\varepsilon_A=\varepsilon_C=1.96$ and $\varepsilon_B=\varepsilon_D=4$, which can be easily realized in materials such as porous silicon [28]. The thicknesses of the layers are, respectively, $d_A=435.5$ nm, $d_B=96$ nm, $d_C=100$ nm, and $d_D=330$ nm. The transmittances are calculated by the transfer-matrix method [26]. Different from the PhC-PhC heterostructures studied in Ref. [7], where the unit cell of one of the PhCs is two times as thick as that of the other PhC in the heterostructure, the unit cell (AB) and unit cell (CD) possess equal optic length, which means that their gaps overlap with each other. We plot $|\xi_\beta^s - \xi_\gamma^s|$ and the transmittance as functions of frequency for heterostructures with $n=9$ and $m=3,7,9,12$, in the frequency range lying in the first gap of both PhCs. The solid lines represent $|\xi_\beta^s - \xi_\gamma^s|$ and the dashed lines are the transmittance of the corresponding heterostructure. Except for the case of $m=3$ where no peak appears in the transmittance and no dip in $|\xi_\beta^s - \xi_\gamma^s|$, the transmission peak appears just at the frequency where $|\xi_\beta^s - \xi_\gamma^s|$ is minimum in anyone of the other three heterostructures.

However, not all of the three transmission peaks for the three heterostructures reach unity. As one can find in Eqs. (13) and (14), the numbers of unit cells in the PhCs play an important role in determining the corresponding surface im-

pedance. For the heterostructure with $m=9$, $n=9$, the surface impedances at two sides of the interface match perfectly with each other, and at the same frequency, there is a perfect transmission. When m varies, the surface impedance ξ_β^s changes, and the matching condition is no longer fulfilled. As shown in Fig. 3, the dips in the lines representing $|\xi_\beta^s - \xi_\gamma^s|$ do not reach exactly 0 for $m=7,12$. As a result, the amplitude of the transmission at the peak frequency in each of these two cases experiences an obvious deviation from unity.

We have demonstrated that the match of the surface impedances [Eq. (15)] can be used as a criterion for the occurrence of OTSs for a PhC-PhC heterostructure. Meanwhile, this criterion is also correct for the occurrence of OTSs in metal-PhC heterostructures, which can be seen from following discussions about the transmittance of a metal-PhC heterostructure that has been experimentally explored in Ref. [17]. The heterostructure is composed with an Au film ($d_m=30$ nm) and a finite PhC $(\mathrm{GaAs/Ga_{0.1}Al_{0.9}As})_{19}$ with $d_{\mathrm{Ga_{0.1}Al_{0.9}As}}=59.3$ nm and $d_{\mathrm{GaAl}}=76.2$ nm. The relevant dielectric constant of Au is represented by the Drude mode involving dispersion and absorption as $\varepsilon_{\mathrm{Au}}=1-\omega_p^2/[\omega(\omega+i\gamma)]$ where ω_p is the plasma frequency, and γ is the plasma collision rate. For Au at room temperature, we take $\omega_p=1.35\times10^{16}$ Hz and $\gamma=4.096\,5\times10^{13}$ Hz [17]. The relevant dielectric constants of GaAs and $\mathrm{Ga_{0.1}Al_{0.9}As}$ are taken from Ref. [29],

$$\varepsilon_j(\omega)=A_j+\sum_{i=0,1}\frac{C_{ji}}{(\hbar\omega)^2-E_{ji}^2}, \tag{16}$$

where A_j ($j=\mathrm{Ga_{0.1}Al_{0.9}As}$, GaAs), C_{ji} ($i=0,1$) are constants, $\hbar\omega$ is the energy of photon, and E_{ji}s are the resonant energies. As the energy of photons is far from any of the resonant energies, the dielectrics in PhCs involve slightly the dispersion. The surface impedance ξ_{Au}^s at the metal side of the interface is calculated by taking $\xi_{1+}^{\mathrm{Bloch}}=-\xi_{1-}^{\mathrm{Bloch}}=\xi_{\mathrm{Au}}$ and $e^{imk_1^B d}=e^{ik_0\sqrt{\varepsilon_{\mathrm{Au}}}d_m}$ in Eq. (13). In Fig. 4 we demonstrate $|\xi_{\mathrm{PhC}}^s-\xi_{\mathrm{Au}}^s|$ and the transmittance of the $\mathrm{Au(GaAs/Ga_{0.1}Al_{0.9}As)_{19}}$ heterostructure. One can find that a transmission peak or an OTS occurs exactly at the frequency where the surface impedances match best. The low transmission at the peak frequency is due to the absorption in the metal. The result is in agreement with the expectancy from the criterion of OTSs by the match of the surface impedances.

In this section, the surface impedance at each side of the interface inside a PhC-PhC heterostructure is calculated by applying the BWEM, and the match of the surface impedances is used to be a criterion of OTSs at PhC-PhC interface or metal-PhC interface. The criterion is demonstrated to be valid by comparison between the transmission peaks and the minimums of the differences of the surface impedances. Although the transmittance can be calculated by the transfer-matrix method, the transfer matrix of a PhC-PhC heterostructure which needs to be calculated layer by layer is very complex and it is difficult to give an analytical criterion for the occurring of a resonant tunneling. In the criterion for OTSs by BWEM [Eqs. (13)–(15)], the PhCs lying on each side of the interface are represented by the parameters de-

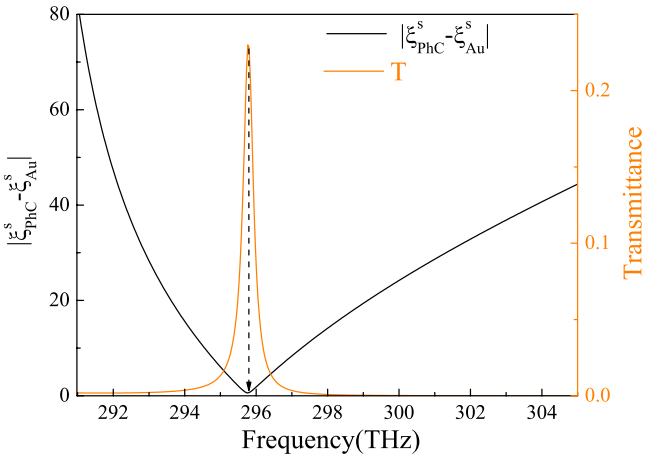

FIG. 4. (Color online) The occurrence of OTSs and the match of surface impedances at the metal-PhC interface of a heterostructure $\mathrm{Au(GaAs/Ga_{0.1}Al_{0.9}As)_{19}}$, where the metal is a 30-nm-thick Au layer. Realistic parameters of the materials are employed.

rived from a single unit cell [Eqs. (3) and (5)] and the number of the unit cells. This will provide us a great convenience in analysis about what kind of finite PhCs can constitute heterostructures that can sustain OTSs.

IV. DISCUSSION AND CONCLUSION

In Sec. III we got the criterion of OTSs by the match of surface impedances at the interface inside a PhC heterostructure. The surface impedance at each side of the interface takes a simple form in the schematic of BWEM as Eq. (13) or Eq. (14) which can be written, respectively, as

$$\xi_\beta^s=\frac{\xi_{1+}(\xi_0-\xi_{1-}^{\mathrm{Bloch}})+\xi_{1-}e^{-2imk_1^{\mathrm{Bloch}}d_1}(\xi_{1+}^{\mathrm{Bloch}}-\xi_0)}{(\xi_0-\xi_{1-}^{\mathrm{Bloch}})+e^{-2imk_1^{\mathrm{Bloch}}d_1}(\xi_{1+}^{\mathrm{Bloch}}-\xi_0)}, \tag{17}$$

$$\xi_\gamma^s=\frac{\xi_{2+}(\xi_0-\xi_{2-}^{\mathrm{Bloch}})+\xi_{2-}e^{2ink_2^{\mathrm{Bloch}}d_2}(\xi_{2+}^{\mathrm{Bloch}}-\xi_0)}{(\xi_0-\xi_{2-}^{\mathrm{Bloch}})+e^{2ink_2^{\mathrm{Bloch}}d_2}(\xi_{2+}^{\mathrm{Bloch}}-\xi_0)}. \tag{18}$$

As the frequency range which we studied lies in the gaps of the PhCs on both sides of the interface, owing to the evanescent nature of Bloch wave, we have $|e^{ik_1^{\mathrm{Bloch}}d_1}|<1$ and $|e^{ik_2^{\mathrm{Bloch}}d_2}|<1$. In the limit case with $m\to\infty, n\to\infty$, i.e., the heterostructure is a combination of two semi-infinite PhCs, we obtain $\xi_\beta^s=\xi_{1-}^{\mathrm{Bloch}}$ and $\xi_\gamma^s=\xi_{2+}^{\mathrm{Bloch}}$. The match of surface impedances turns to be the match of eigenimpedances and the EM wave inside each semi-infinite PhC is just a single eigen-Bloch wave. It is consistent with the analysis in Refs. [7,11]. When the numbers of unit cells in each PhC are not large, the surface impedance at the interface is quite different from the Bloch impedance of the infinite PhC. The match of Bloch impedances $|\xi_{1-}^{\mathrm{Bloch}}-\xi_{2+}^{\mathrm{Bloch}}|=0$ is not suitable for the prediction of OTSs. In Fig. 5(a), as a function of frequency, $|\xi_{1-}^{\mathrm{Bloch}}-\xi_{2+}^{\mathrm{Bloch}}|$ is given in the gap of both semi-infinite PhCs. Figure 5(b) shows the transmittances through three finite heterostructures embedded in air. There is a peak of unity for each of three heterostructures, which indicates the occur-

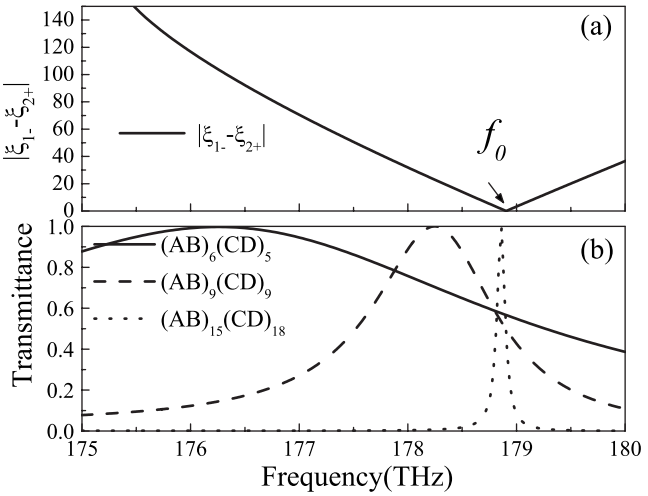

FIG. 5. Comparisons between the match of eigenimpedances and the OTSs in finite heterostructures. f_0 labeled in (a) is the frequency where the eigenimpedances ξ_{1-} and ξ_{2+} match best. The solid, dash, and the dot lines in (b) are, respectively, the transmittances of $(AB)_6(CD)_5$, $(AB)_8(CD)_8$, and $(AB)_{15}(CD)_{18}$.

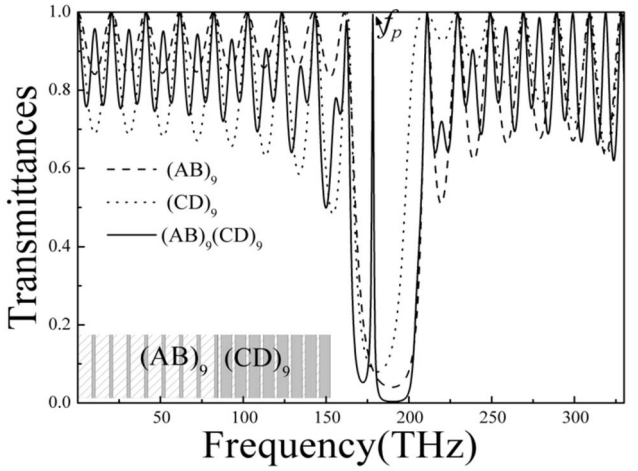

FIG. 6. The transmittances of $(AB)_9(CD)_9$, $(AB)_9$, and $(CD)_9$. The substrate is air. The inset shows schematically the heterostructure.

rence of an OTS at the corresponding frequency. One can see that the frequencies of the peaks in the three finite heterostructures are quite different with the infinite case. The less the periods, the farther the frequency of OTSs shifting away from f_0 where $|\xi_{1-}^{\text{Bloch}}-\xi_{2+}^{\text{Bloch}}|=0$. Furthermore, the transmission coefficients at the frequency f_0 for all these three heterostructures are much lower than unity. Thus one can find that the eigenimpedance matching occurrence criterions for OTSs cannot be used to finite PhC heterostructures. In the criterion of OTSs by the match of surface impedance given by Eqs. (13)–(15), the numbers of periods of both PhCs m and n are well considered, which provides us the feasibility of accurate predictions about OTSs in finite heterostructures.

Reference [7] has studied the OTSs at the interface between two PhCs; one of which has a period close to the wavelength of light and the other one has a period close to the double of the wavelength. It was demonstrated that (i) OTSs can occur in the frequency range lying in the odd gap of one PhC and even gap of the other and (ii) the order of the slabs at the interface has a crucial effect on the OTSs. When the PhCs at the right-hand side of the interface begins with a low index slab, the structure can sustain OTSs. When the order of the elements of the PhCs is changed and with a high index layer adhering to the interface at the right-hand side of the interface, the OTSs disappear.

Different from the descriptions about OTSs in Ref. [7], we find that OTSs are not necessarily in the frequency range lying in the odd gap of one PhC and even gap of the other PhC in the heterostructure. OTSs can also exist at the frequency lying in the first gap of both constituting PhCs, which can be seen from Fig. 6, where the transmittances for $(AB)_9(CD)_9$, $(AB)_9$, and $(CD)_9$ embedded separately in air are plotted, respectively, by solid, dashed, and dotted lines. In Fig. 7, we demonstrate the transmittances and the matches of the surface impedances of four heterostructures with properly chosen m and n. One can find that by choosing proper sets of m and n, $(AB)_m(CD)_n$, $(AB)_m(DC)_n$, $(BA)_m(CD)_n$, and $(BA)_m(DC)_n$ can all sustain resonant tunnelings and thus OTSs. Just as we have demonstrated, it is the match of surface impedances at different sides of the interface that determines the occurrence of the OTSs. When the unit-cell configuration of one of the PhCs changes such as from (AB) to (BA) or from (CD) to (DC), the eigenimpedances [Eq. (5)] and thus the surface impedance [Eq. (13) or Eq. (14)] at the corresponding side of the interface changes critically. So the order of the unit-cell configuration will surely affect the occurrence of OTSs. But there seems no inevitable link between the orders of the elements in the unit cells and the occurring of OTSs.

In conclusion, a Bloch-wave-expansion method is introduced to study the transmission properties of finite PhCs. We demonstrated that a finite PhC can be characterized by two Bloch impedances and the Bloch-wave vector in the Bloch–wave-expansion method where both the periodicity and the

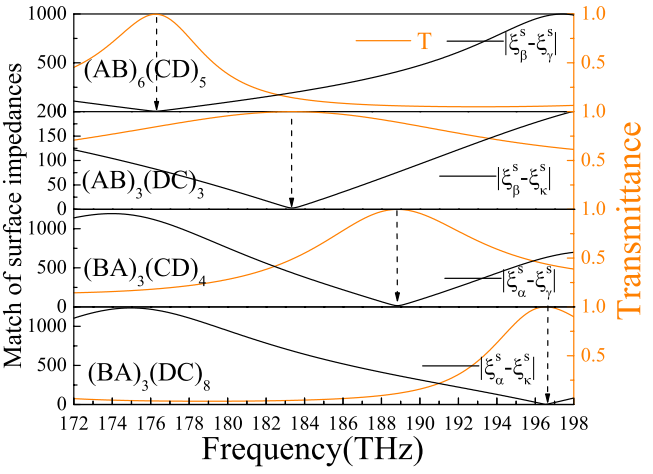

FIG. 7. (Color online) Resonant tunnelings and the matches of the surface impedances for four kinds of heterostructures $(AB)_6(CD)_5$, $(AB)_3(DC)_3$, $(BA)_3(CD)_4$, and $(BA)_3(DC)_8$.

symmetry of PhCs are considered fully. Applying the method to PhCs in a heterostructure, we obtained the relation of fields at different boundaries of the PhCs inside the heterostructure and gave a criterion for the occurrence of optic Tamm states in the heterostructure by the match the surface impedances at the different sides of the interface. It is expected to give some instructions to the search of PhC heterostructures which can sustain OTSs.

ACKNOWLEDGMENTS

This work was supported by National Natural Science Foundation of China under Grants No. 10874129 and No. 10634050, National Basic Research Program (973) of China under Grant No. 2006CB921701, and Shanghai Science and Technology Committee under Grants No. 08dj1400300 and No. 07dz22302.

[1] S. Kawata, *Near-Field Optics and Surface Plasmon Polaritons* (Springer, Berlin, 2001).
[2] E. A. Stern and R. A. Ferrell, Phys. Rev. **120**, 130 (1960).
[3] H. Raether, *Surface Plasmon on Smooth and Rough Surfaces and on Gratings* (Springer-Verlag, Berlin, 1988).
[4] E. Altewischer, M. P. van Exter, and J. P. Woerdman, Nature (London) **418**, 304 (2002).
[5] M. M. Baksh, M. Jaros, and J. T. Groves, Nature (London) **427**, 139 (2004).
[6] W. L. Barnes, A. Dereux, and T. W. Ebbesen, Nature (London) **424**, 824 (2003).
[7] A. V. Kavokin, I. A. Shelykh, and G. Malpuech, Phys. Rev. B **72**, 233102 (2005).
[8] A. Kavokin, I. Shelykh, and G. Malpuech, Appl. Phys. Lett. **87**, 261105 (2005).
[9] T. Goto, A. V. Dorofeenko, A. M. Merzlikin, A. V. Baryshev, A. P. Vinogradov, M. Inoue, A. A. Lisyansky, and A. B. Granovsky, Phys. Rev. Lett. **101**, 113902 (2008).
[10] B. J. Lee, Y. Chen, and Z. M. Zhang, Opt. Lett. **33**, 204 (2008).
[11] A. P. Vinogradov, A. V. Dorofeenko, S. G. Erokhin, M. Inoue, A. A. Lisyansky, A. M. Merzlikin, and A. B. Granovsky, Phys. Rev. B **74**, 045128 (2006).
[12] M. Kaliteevski, I. Iorsh, S. Brand, R. A. Abram, J. M. Chamberlain, A. V. Kavokin, and I. A. Shelykh, Phys. Rev. B **76**, 165415 (2007).
[13] J. Barvestani, M. Kalafi, A. Soltani-Vala, and A. Namdar, Phys. Rev. A **77**, 013805 (2008).
[14] I. A. Shelykh, M. Kaliteevskii, A. V. Kavokin, S. Brand, R. A. Abram, J. M. Chamberlain, G. Malpuech, Phys. Status Solidi A **204**, 522 (2007).
[15] A. Namdar, I. V. Shadrivov, and Y. S. Kivshar, Appl. Phys. Lett. **89**, 114104 (2006).
[16] A. Namdar, I. V. Shadrivov, and Y. S. Kivshar, Phys. Rev. A **75**, 053812 (2007).
[17] M. E. Sasin, R. P. Seisyan, M. A. Kalitteevski, S. Brand, R. A. Abram, J. M. Chamberlain, A. Yu. Egorov, A. P. Vasil'ev, V. S. Mikhrin, and A. V. Kavokin, Appl. Phys. Lett. **92**, 251112 (2008).
[18] J. Guo, Y. Sun, Y. Zhang, H. Li, H. Jiang, and H. Chen, Phys. Rev. E **78**, 026607 (2008).
[19] D. R. Smith, D. C. Vier, Th. Koschny, and C. M. Soukoulis, Phys. Rev. E **71**, 036617 (2005).
[20] A. Alu and N. Engheta, IEEE Trans. Antennas Propag. **51**, 2558 (2003).
[21] I. Vorobeichik, M. Orenstein, and N. Moiseyev, IEEE J. Quantum Electron. **34**, 1772 (1998).
[22] A. M. Kennis, I. Vorobeichik, and N. Moiseyev, IEEE J. Quantum Electron. **36**, 563 (2000).
[23] J. D. Joannopoulos, S. G. Johnson, R. D. Meade, and J. N. Winn, *Photonic Crystals: Molding the Flow of Light*, 2nd ed. (Princeton Univeristy Press, Princeton, 2008).
[24] P. Yeh, A. Yariv, and C. Hong, J. Opt. Soc. Am. **67**, 423 (1977).
[25] A. Figotin and V. Gorentsveig, Phys. Rev. B **58**, 180 (1998).
[26] M. Born and E. Wolf, *Principles of Optics: Eletromagnetic Theory of Propagation, Interference and Diffraction of Light*, 6th ed. (Pergamon, Oxford, 1980).
[27] J. Perruisseau-Carrier, A. K. Skrivervik, and I. E. T. Microw, IET Proc. Microwaves, Antennas Propag. **1**, 50 (2007).
[28] V. Agarwal, J. A. del Rio, G. Malpuech, M. Zamfirescu, A. Kavokin, D. Coquillat, D. Scalbert, M. Vladimirova, and B. Gil, Phys. Rev. Lett. **92**, 097401 (2004).
[29] S. Gehrsitz, F. K. Reinhart, C. Gourgon, and N. Herres, J. Appl. Phys. **87**, 7825 (2000).